ELSEVIER

Carbohydrate Polymers 42 (2000) 159–174

Carbohydrate Polymers

www.elsevier.com/locate/carbpol

Characterisation of xanthan gum solutions using dynamic light scattering and rheology

A.B. Rodd[a], D.E. Dunstan[b,*], D.V. Boger[a]

[a]*Department of Chemical Engineering, The University of Melbourne, Parkville 3052, Australia*
[b]*Cooperative Research Centre for Industrial Plant Biopolymers, The University of Melbourne, Parkville 3052, Australia*

Received 30 September 1998; received in revised form 26 August 1999; accepted 15 September 1999

Abstract

The 'weak gel' formation mechanism of xanthan gum solutions has been examined using rheological and light scattering methods. Significant differences are observed between the critical overlap concentration (c^*) measured using both techniques. The effect of shear on c^* for semi-flexible molecules such as xanthan is demonstrated. The approximate theories of Doi and Edwards ((1984). The Theory of Polymer Dynamics. Oxford: Clarendon Press) for rigid rods and De Gennes ((1979). Scaling Concepts in Polymer Solutions. London: Cornell University Press) for random coils are used to explain the differences observed between rheological and light scattering measurements of c^*. A second concentration regime parameter due to aggregation, c^{**}, is observed in dynamic light scattering results (DLS). The parameter c^{**} has been previously observed for xanthan systems. Light scattering measurements in various electrolytes suggest that the use of DLS is able to distinguish between the transition from truly dilute behaviour to semi-dilute behaviour (c^*) and the critical concentration for aggregation (c^{**}).

Keywords: Xanthan; Light scattering; Coil overlap concentration

1. Introduction

Xanthan gum is a high molecular weight extracellular polysaccharide produced by bacteria of the genus *Xanthomonas*. Commercial xanthan gum is extracted from *Xanthomonas campestris*. However, for the purpose of most scientific studies, it is extracted from *Xanthomonas phaseoli* and *Xanthomonas juglandis*. Xanthan gum may be chemically considered as an anionic polyelectrolyte, with a backbone chain consisting of (1 → 4)β-D-glucan cellulose. The polymer backbone is substituted at C-3 on alternate glucose residues with a trisaccharide sidechain. The sidechain consists of β-D-mannopyranosyl-(1 → 4)-(α-*d*-glucuropyranosyl)-(1 → 2)-β-*d*-mannopyranoside 6-acetate. A pyruvic acid residue is linked to the 4 and 6 positions between 31–56% of the terminal D-mannose residues (Morris, Morris & Ross-Murphy, 1982; Rinaudo & Milas, 1980; Ross-Murphy, Morris & Morris, 1983). The xanthan molecule undergoes a conformation transition from an ordered double helix to a random coil when heated to above, between 40 and 80°C depending on the ionic strength of solution (Paradossi & Brant, 1982; Sato, Norisuye & Fujita, 1984). The ordered conformation of the xanthan molecule is semi-flexible with a hydrodynamic length varying between 600 and 2000 nm (Holzwarth, 1978; Ross-Murphy et al., 1983) and a hydrodynamic diameter of the order of 2 nm (Stokke, Elgsaeter & Smidsrod, 1986). A number of workers have investigated the degree of flexibility of the xanthan molecule, generally characterised in terms of persistence length (L_p). Static light scattering and sedimentation coefficients were used with application of the Benoit and Doty (1953) expansion of the Krakty Porod model for a wormlike chain to predict the flexibility (Richards, 1980). Experimental measurements of the persistence length have yielded values which vary between 130 ± 20 nm (Berth, Dautzenburg, Christensen, Harding, Rother & Smidsrod, 1996; Sato et al., 1984) or 45–70 nm (Muller, Lecourtier, Chauveteau & Allain, 1984; Tinland, Maret & Rinaudo, 1990; Tinland & Rinaudo, 1989). The two regions of L_p determined suggest that thermal history and xanthan source are important parameters in considering the flexibility of xanthan molecules and its behaviour in solution.

Solutions of xanthan gum are one of the most intensively studied polysaccharide systems both in terms of rheological properties and physical chemistry. The behaviour of xanthan in both dilute and semi-dilute solutions has been

* Corresponding author.
E-mail address: d.dunstan@chemeng.unimelb.edu.au (D.E. Dunstan).

0144-8617/00/$ - see front matter
PII: S0144-8617(99)00156-3

extensively studied (Carriere, Amis, Schrag & Ferry, 1993; Coviello, Kajiwara, Burchard, Dentitni & Crescenzi, 1986; Coviello, Burchard, Dentini & Crescenzi, 1987; Southwick, Jamieson & Blackwell, 1981; Tinland et al., 1990; Whitcomb & Macosko, 1978;). The determination of concentration regimes is an important aspect of previous work and illustrates the complicated nature in which xanthan behaves in solution. The concentration at which individual polymer molecules begin to physically interact is defined as c^*. The concept of c^* is based on the theory that the polymer coils in solution in their quiescent state occupy a hydrodynamic volume where above a critical concentration for close packing the molecules interact. DLS may be used to trace the diffusivity of molecules in solutions through a range of concentrations and gain insight into the solutions behaviour in a truly dilute environment. c^* has been evaluated by application of light scattering techniques through analysis of trends in apparent diffusion coefficients (Coviello et al., 1987; Tinland et al., 1990).

Rheologically, c^* of polymer solutions is determined by extrapolation of shear viscosity data to zero shear viscosities over a range of concentrations. On a double logarithmic plot of zero shear viscosity versus concentration, a slope of approximately one in the dilute regime and between three and four in the semi-dilute regime is observed, depending on the rigidity of the molecule (Lapasin, Pricl, Paoletti & Zanetti, 1990). The concentration at which the slope of zero shear viscosity versus concentration changes, is defined as c^*. A limitation of the rheological measure of c^* is the measure of zero shear viscosities which involves the application of shear to the system. In the case of solutions of xanthan gum, shear forces will dominate Brownian motion at low shear rates, causing molecular alignment, resulting in the solution not being in a state of true random motion and Rotary Peclet Numbers >1 (Lapasin & Pricl, 1993). Doi and Edwards (1984) show theoretically that under the application of shear forces, rod-like molecules will align in solution and move longitudinally in a constrained tube before molecular interaction occurs. Although xanthan molecules may not be considered as rodlike (Coviello et al., 1987), their extended form in solution suggests the alignment of molecules in solution may be applied qualitatively.

Because of the semi-flexible nature of xanthan and the tendency for aggregation or self-association at low concentrations, it is difficult to obtain a measure of c^* when shear is applied (Kojima & Berry, 1988; Tinland et al., 1990). Southwick et al. (1981) applied quasi elastic light scattering to solutions of xanthan gum and determined a c^* of 0.02 wt%. Their calculations assumed sphericity and the authors speculated a much lower value to be more indicative of the initial concentration for molecular overlap. Southwick et al. (1981) observed a second transition at 0.07 wt% where a general decrease in relaxation times and the onset of bimodal behaviour occurs, which was attributed to the onset of anisotropy. Bimodal behaviour is defined as having two distinct diffusion coefficients. Jamieson, Southwick and Blackwell (1982) applied static light scattering through a range of concentrations and observed a discontinuity of translational diffusion at 0.02 wt%, interpreted as the onset of the semi-dilute regime, however, no diffusion plateau consistent with Stokes–Einstein measure of diluteness was observed. The workers also observed a linear relationship between intensity and concentration for flow birefringence of xanthan solutions with a concentration above 0.1 wt%. This observation agrees qualitatively, but not quantitatively with the predictions of Doi and Edwards (1984) for an anisotropic entangled solution of rigid-rod molecules.

Coviello et al. (1986) examined dynamic and static light scattering from native and modified xanthan and commented on the ambiguity in determining c^* for semi-flexible objects, suggesting that the value obtained is often dependent on experimental technique and interpretation of the data. Tinland et al. (1990) comment on the reptation of semidilute solutions of worm-like polymers and report a c^* of 0.04 wt% for xanthan gum of a similar molecular weight to that reported here from deviation of the self diffusion coefficient as measured through DLS.

Milas, Rinaudo, Knipper and Schuppsier (1990) applied steady shear and dynamic rheological measurements to an unpasteurized sample of xanthan gum, and through sensitive rheological measurements observed two concentration transitions which were assigned c^* and c^{**}. These workers observed a departure from a slope of one of the specific viscosity versus $c\cdot[\eta]$ (concentration times intrinsic viscosity) at 0.126 wt%. A similar value was also obtained by applying large deformation rheology where a departure from Newtonian behaviour to pseudoplastic behaviour was observed. A second concentration transition was assigned c^{**} and observed at 0.60–0.78 wt%. c^{**} was assigned to the concentration where specific viscosity followed $(c\cdot[\eta])^{3.7}$ which is similar to that observed for polymeric melts. Milas et al. (1990) speculate that c^{**} represents the onset of a concentrated domain in which a uniform distribution of polymer segments is present. Other workers have expanded on the concept of c^* and c^{**}, by applying complementary rheooptical techniques of birefringence and dichroism to commercial xanthan gum samples. A steady state orientation angle after shearing was observed for samples with a concentration of 0.2 wt% or greater using dichroism. Although the presence of aggregates was observed down to concentrations of 50 ppm, no steady state orientation was observed (Meyer, Fuller, Clark & Kulicke, 1993). The presence of aggregates at such low concentrations is consistent with the observations of Jamieson et al. (1982).

For the most part, previous determinations of c^* and c^{**} have involved combination of two or more experimental techniques and/or the application of shear to solutions of xanthan gum. DLS is a non purtabative technique commonly used to measure the diffusion of polymer molecules in solution and has been used in the present study for the determination of both c^* and c^{**}. DLS

measures a diffusion coefficient which has dimensions of (length)^2/time and is a space average measure of an individual molecules diffusional path which is interpreted by analysis of time correlation functions (TCF).

Light scattering of xanthan gum solutions is complicated by the semi-flexible nature of the xanthan molecules proposed to be a right hand double helix (Bezemer, Ubbink, deKooder, Kuil & Leyter, 1993; Milas, Rinaudo, Duplessix, Borsali & Lindner, 1995) and the presence of micro-aggregates at low concentrations caused by xanthan gum self-association (Meyer et al., 1993). Increased rigidity of the xanthan ordered conformation at higher salt conditions by the reduction of the electrical double layer, suggests that the hydrodynamic radius of an individual molecule would increase as electrolyte is added. Self-association processes in xanthan solutions complicates this hypothesis through the introduction of large aggregates at low concentrations enabling molecules to interact at lower concentrations than would be theoretically expected for a solution of semi-flexible non-interacting molecules (Ferry, 1980).

The work presented here aims to examine xanthan solutions using both rheological techniques and DLS in order to characterise the boundary between dilute and semi-dilute solutions. Experiments have been conducted to quantify c^* and c^{**} as defined by previous work (Meyer et al., 1993; Milas et al., 1990; Southwick et al., 1981) in the absence of shear. The results have been compared with shear rheology data and theoretical calculations. Varying electrolyte concentrations have been used to determine the effect of electrostatic screening on the light scattering and rheological data. The effect of heat treatment on xanthan solutions has been investigated to establish the effect of removing molecular aggregates by converting the xanthan molecule into its re-natured form ensuring a true molecular dispersion (Capron, Brigand & Muller, 1997). The high aspect ratio of xanthan molecules in solution requires characterisation of the effect of different lengths of the scattering vector (**K**) on the xanthan molecule diffusion (Berth et al., 1996; Gamini & Mandell, 1994). The observed diffusional trends have been compared with theoretical predictions of rigid rods in solution (Doi & Edwards, 1984) and scaling concepts for random coils (De Gennes, 1979).

2. Experimental

2.1. Xanthan

The commercial food grade xanthan (Keltrol, lot no PX67769) was provided by Keltrol, USA. It was determined as having a molecular weight of approximately 3.4×10^6 g/mol and a polydispersity of 1.12 as measured using Size Exclusion Chromatography (SEC). In addition, a preliminary static light scattering study yielded a persistence length of 44 nm by application of the Benoit and Doty modification of the Krakty Porod model for a worm-like coil (Benoit & Doty, 1953). It is speculated that, as xanthan was not dialysed to a single counterion form, aggregates may be present for the SEC study giving an overestimate of the molecular weight, however agreement with previous work is observed (Berth et al., 1996; Dhami, Harding, Jones, Hughes, Mutchell & To, 1995; Gamini & Mandell, 1994; Tinland et al., 1990). An average moisture content of 13.272 ± 0.29 wt % was obtained using a Sartorius balance—model MA30-000V2.

2.2. Solution preparation

Xanthan gum solutions were prepared in 1-litre batches using the appropriate electrolyte. The samples were hydrated for 24 h before being stored until use at 4°C to minimise bacterial growth (Chauveteau, 1982). Analytical grade sodium chloride and potassium chloride solutions were prepared and filtered using 0.22 μm filters. All salt solutions were refrigerated at 4°C until use. The effect of thermal treatment on xanthan solutions was investigated by heating individual dilutions of xanthan at 80°C for 2 h. Milas et al. (1990) observed considerable lowering of the values of c^* and c^{**} after heat treatment of xanthan solutions at 80°C for 1 min. Prior investigation into the effect of heat treatment on xanthan solutions has shown that thermal treatment has a considerable effect on the rheological properties (Capron et al., 1997; Milas, Reed & Printz, 1996). In addition to filtration three times through a 0.22 μm filter, xanthan solutions used in DLS were centrifuged at 15 000 g for 2 h directly before use to ensure no bacteria were present (Wilkins et al., 1993).

2.3. Rheometry

The experiments reported here were performed on a Carrimed CSL100 controlled stress rheometer. A cone and plate geometry was used to ensure a constant shear rate in the sample. A 6 cm cone with an angle of $1'59''$ and a truncation of 52 μm was used in all experiments. For a $2'$ cone angle, the variation in shear rate across the gap was calculated to be 0.21% (Barnes, Hutton & Walters, 1989). The stress range of the Carrimed with this measurement system was 1.8×10^{-3}–40 Pa, which allowed accurate determination of the low shear Newtonian plateau by a shear stress ramp for all concentration ranges measured. Equilibrium flow measurements were performed for higher concentration samples to extend the accuracy of the low-end range.

2.4. Dynamic light scattering

Light scattering measurements were conducted on a Malvern Series 4700 Spectrometer, using a 488 nm Argon Ion laser operating at 10 mW. All measurements were conducted at 25°C and a solvent viscosity of 0.890 cp was assumed.

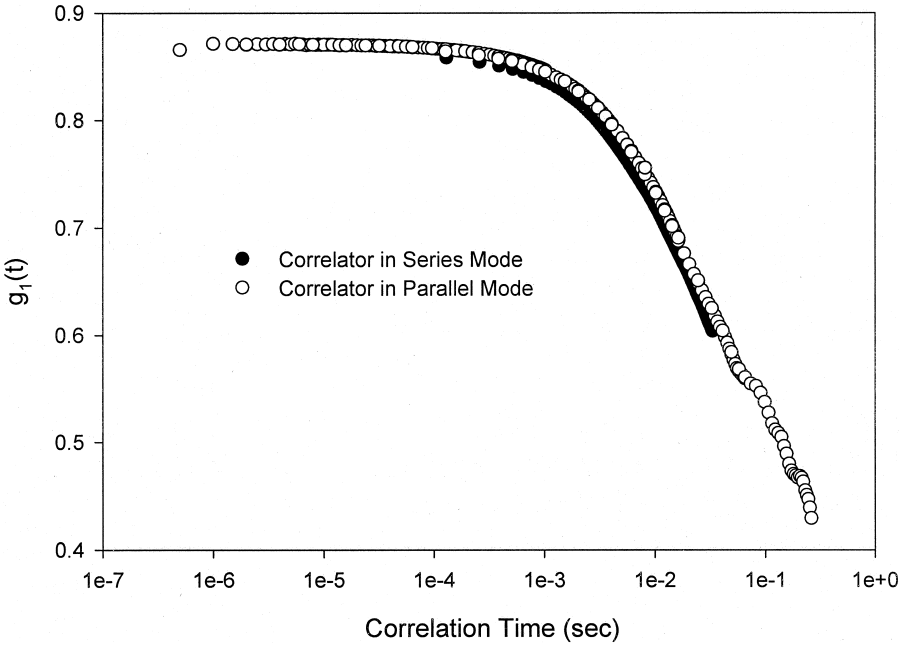

Fig. 1. Correlation function for both series and parallel modes for xanthan at a concentration of $c = 0.1236$ wt% in 15 000 ppm NaCl and at a scattering angle of $\theta = 40°$. The normalised TCF, $g_1(\tau)$ has been converted to $g_2(\tau)$ using the Siegert relationship and an experimentally predicted baseline value.

In DLS measurements a detector is connected to an auto-correlator, and time variations in the scattered intensity, $I(t)$ resulting from the translation diffusion of molecules is measured to give the time correlation function (TCF), $G_2(t) = \langle i(0) \times i(t) \rangle$ (Pecora & Berne, 1976). The second-order autocorrelation function $g_2(t)$ in its normalised form is given by:

$$g_2(t) = \frac{\langle I(t) \times I(t+\tau) \rangle}{\langle I(t) \rangle^2} \tag{1}$$

where τ is the delay time and the brackets represent a time average. The measured autocorrelation function is normalised by the experimental baseline intensity A to give the theoretical field autocorrelation function, $g_1(\tau)$ by the Siegert relationship (Pecora & Berne, 1976):

$$g_2(\tau) = A + B \times |g_1(\tau)|^2, \tag{2}$$

where B is a constant dependent on the optics of the system. It is common to analyse the data by fitting a normalised second-order auto correlation function $g_1(\tau)$ to the equation (Galinsky & Burchard, 1996; Koppel, 1972; Southwick et al., 1981):

$$g_1(\tau) = [a_1 \exp(-K^2 D_1 \tau) + a_2 \exp(-K^2 D_2 \tau)]^2 + b, \tag{3}$$

where a_i is the intensity amplitude of the particle population with a diffusion coefficient of D_i and $b = 1$. In the case of two diffusive processes occurring, they are allocated as being D_{fast} and D_{slow}. The molecular interpretation of fast and slow diffusive processes is still the subject of debate (Mathiez, Mouttet & Weisbuch, 1980). $\bar{\Gamma}$ is the cumulunt to which a diffusion coefficient D is related by:

$$\bar{\Gamma}(K) = D(K) \times K^2 \tag{4}$$

and K is the particle scattering vector given by:

$$|K| = (4\pi n/\lambda_0) \cdot \sin(\theta/2) \tag{5}$$

where λ_0 is the wavelength of the laser, n is the solution refractive index and θ is the refractive index.

CONTIN is a general program package suitable for solving linear integral operators and systems of linear algebraic equations (Provencher, 1979; Provencher, 1982). The CONTIN package fits a multi exponential curve to the time correlation function similar in form to Eq. (3). Unfortunately, CONTIN is not able to provide the entire relaxation spectrum, unlike the nonlinear analysis used by Coviello and Burchard (1997). Fig. 1 illustrates a typical auto-correlation function for 0.12 wt% xanthan in 15 000 ppm measured at 25°C and a scattering angle of $\theta = 40°$ showing the superposition of the log and linear curves.

Because of the appearance of a large range of relaxation times, it may be necessary to obtain a correlation function that accurately characterises behaviour over a number of magnitudes of correlation times. To achieve logarithmically spanning correlation functions it is necessary to operate a correlator in both parallel and series modes. 256 channels are present which may be either linearly spaced or split into up to eight sub-correlators each of which contain an equal number of channels that are spaced linearly over different timescales.

In series mode (linear mode/single τ), the channels are linearly separated and a sample time may be chosen and is

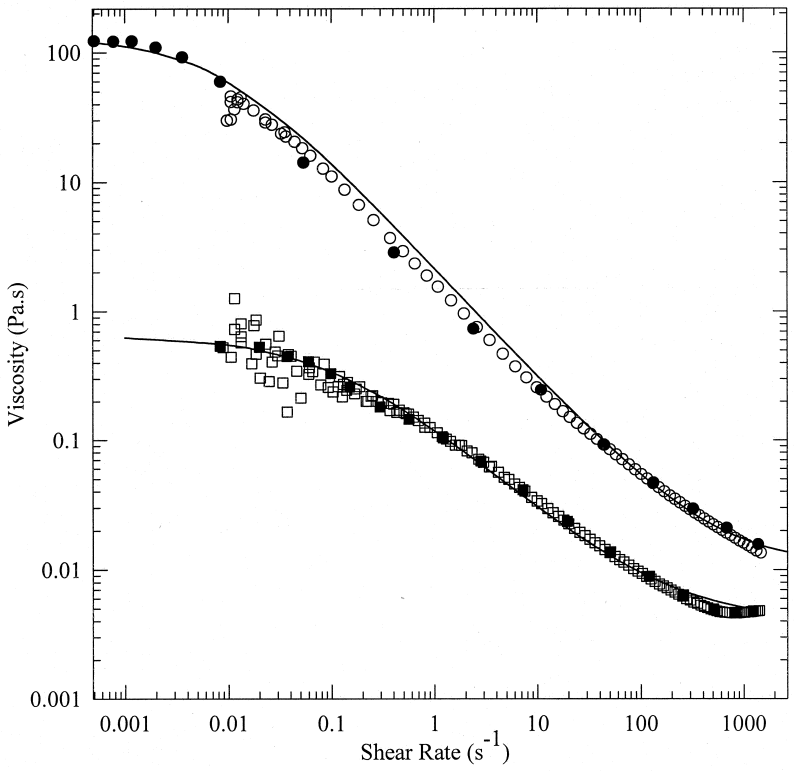

Fig. 2. Viscosity versus shear rate (equilibrium flow ramps and shear rate ramps) for two xanthan concentrations. Circles represent 0.55 wt% and squares represent 0.05 wt%. Equilibrium flow ramps (closed symbols) allows the sample to equilibrate at each applied stress. Shear rate ramps (open symbols) apply a steadily increasing stress to the solution and continually measure the resultant shear rate. Lines represent the fit of cross model given by Eq. (6).

typically in the range of τ— 4–20 μs for the work presented here. Every store channel starts at one sample time later than the preceding one.

In parallel mode (log mode/multi τ) the correlator was split up into eight sub-correlators over which the 256 channels were distributed evenly. Each sub-correlator then samples linearly across a number of channels with a different initial sample time. The sample times vary as τ_1, $d\tau_1$, $d^2\tau_1$, $d^3\tau_1$,… $d^7\tau_1$ depending on the number of sub-correlators used. τ_1 is the shortest sampling time and d is the dilation factor by which the sample times in the other correlators are varied, typically set to between 4 and 6. To avoid saturation of data, pre-scale factors are applied to each of the store subdivisions and vary between 1 and 256. They can be chosen automatically or entered manually, in which case they commonly follow the series, 2, 4, 8, 16, 32, 64, 128 and 256 for the case of 8-sub-correlators. The sample times available are dependent on the correlator settings and, in this work, varied between 0.5 and 6.4 μs.

3. Results and discussion

Determination of c^* using rheological methods has been conducted by measurement of a range of xanthan concentrations with varying electrolyte conditions. Shear stress ramps were conducted for a range of polymer concentrations in each of the electrolyte conditions. For a number of concentrations, equilibrium flow measurements were conducted in addition to shear stress ramps. Equilibrium flow measurements apply a step increasing stress allowing the shear rate to equilibrate at each applied stress before a measurement is taken. The equilibrium flow measurements enable the determination of a low shear Newtonian plateau for more dilute samples whilst enabling the presence of time effects at higher concentrations to be observed. Fig. 2 illustrates the comparison of equilibrium flow and shear stress ramps for a number of concentrations. Zero shear Newtonian viscosities were interpreted using a Cross Model as shown in Eq. (6).

$$\eta = (\eta_0 - \eta_\infty)/(1 + K\dot{\gamma}^n) + \eta_\infty, \quad (6)$$

where η_0 is the low shear Newtonian viscosity η_∞ is the estimated infinite shear rate Newtonian viscosity, $\dot{\gamma}$ is the shear rate, K is the consistency index and n is the power law index.

Both increasing and decreasing shear stress ramps were conducted on the same solution to check for hysteresis, as seen in Fig. 3. Fig. 4 illustrates the zero shear Newtonian viscosities plotted versus concentration for each electrolyte concentration. The plot shows c^* as indicated by the intersection in the linear fits to both regions. A range of values from 0.065 wt% for 0.1 M KCl solutions to 0.13 wt% for a solution in distilled water was observed. The slope in the

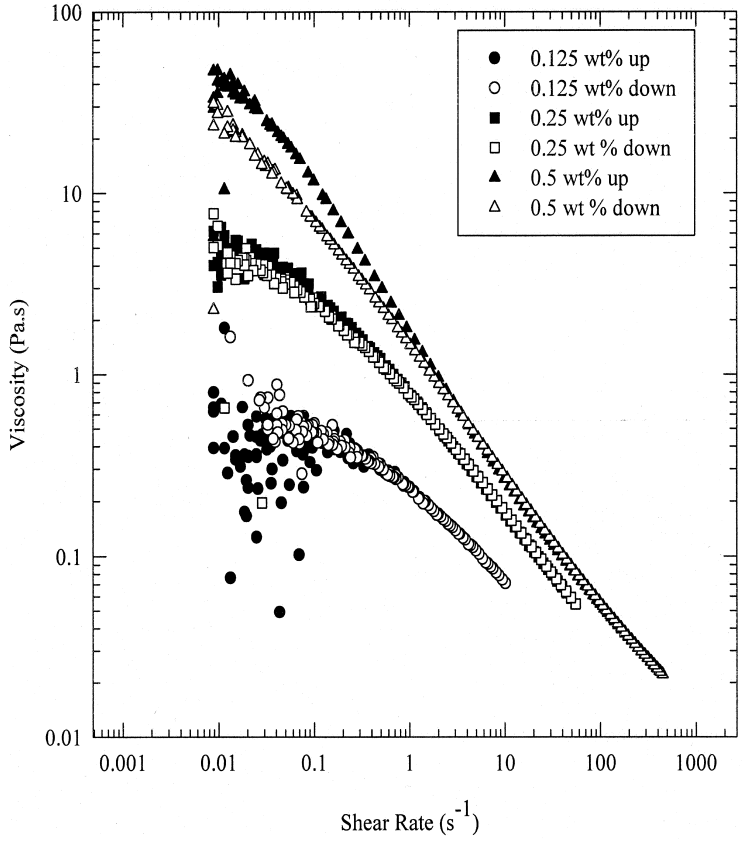

Fig. 3. Viscosity versus shear rate ramps for concentrations of 0.125, 0.25 and 0.5 wt% in DW. Increasing and decreasing shear rate ramps are conducted as a check for hysteresis in the system.

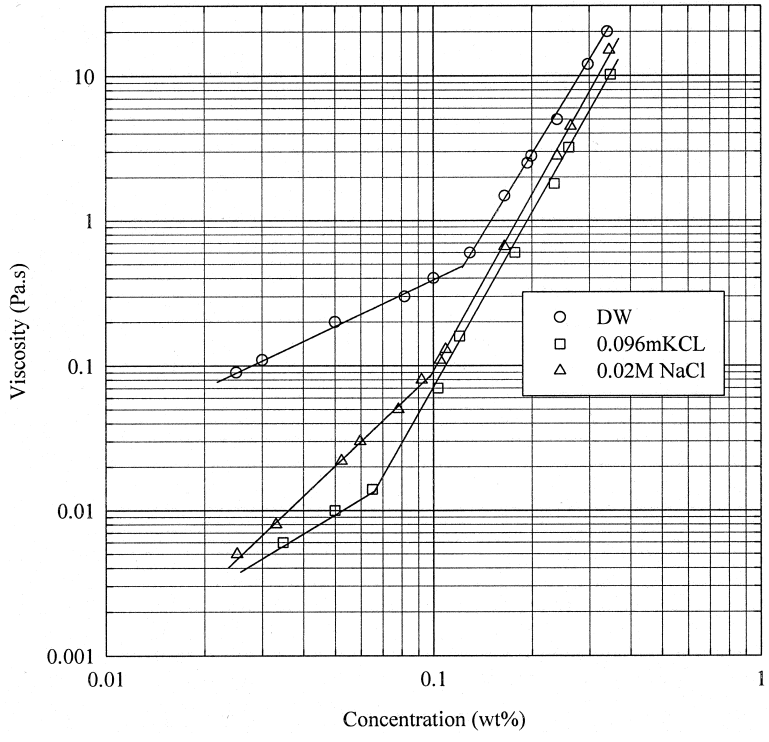

Fig. 4. Extrapolated zero shear Newtonian viscosity versus concentration for xanthan in DW, 0.1 M KCl and 0.02 M NaCl. Discontinuity indicates the rheologically predicted value of c^*.

Table 1
Coil overlap concentration (c^*) for xanthan solutions in three electrolyte conditions. Comparison with calculations based on Krakty–Porod Wormlike coil and a rigid rod molecule, by application of Berry and Russels's (1987) measure of diluteness for rigid molecules. DLS results based on a 5% deviation from infinitely dilute Stokes–Einstein behaviour

Electrolyte conditions (ppm NaCl)	$nl^3 = 1$ for l derived from Worm-like coil Eqs. (12) and (13) (wt%)		$nl^3 = 1$ for l derived from rigid rods Eqs. (7) and (9) (wt%)	Deviation from Inf. dilute behaviour (DLS) (wt%)
	$L_p = 120$ nm	$L_p = 45$ nm		
15000	$\approx 2.45 \times 10^{-3}$	$\approx 9.5 \times 10^{-3}$	11.1×10^{-05}	9×10^{-05}
10000	$\approx 2.45 \times 10^{-3}$	$\approx 9.5 \times 10^{-3}$	4.72×10^{-05}	5×10^{-05}
5000	$\approx 2.45 \times 10^{-3}$	$\approx 9.5 \times 10^{-3}$	3.34×10^{-05}	3×10^{-05}

dilute region varied between 1 and 1.8 depending on electrolyte and was approximately 4.0 in the semi-dilute region (independent of electrolyte conditions). The observed slopes are in agreement with literature values which show the slope in the dilute region to vary between 1.07 and 1.3 and the semi-dilute region is reported to vary from 3.9 to 4.2 (Gravanis, Milas, Rinaudo & Tinland, 1987; Milas & Rinaudo, 1986).

3.1. Theoretical predictions of c^*

It is well known that the conformation of a polymer in solution has an important effect on c^* and should be considered when making theoretical predictions of this quantity. For the case of rigid rods in solution, deviation from dilute behaviour can be expected when the number of molecules in solution is such that the effective hydrodynamic volumes occupied by rods rotating in true Brownian motion overlap. Berry and Russel (1987) developed the following definition:

$$n^* L^3 = 1, \tag{7}$$

where n^* is the number density of polymer molecules in solution and L is the hydrodynamic length of a single molecule in solution. The number density at the point where only one chain occupies one equivalent volume may be related to concentration by the simple conversion:

$$n^* = c^* \times Na_v/M_w, \tag{8}$$

where c^* is the critical concentration Na_v is Avagadro's number and M_w is the polymer molecular weight. For rigid rods in solution the hydrodynamic length (L) can be obtained from the hydrodynamic radius by the relationship (Broersma, 1960):

$$R_h = \frac{L}{2\sigma - 0.19 - \dfrac{8.24}{\sigma} + \dfrac{12}{\sigma^2}}, \tag{9}$$

where $\sigma = \ln(L/r)$, r being the cross-sectional radius. The hydrodynamic radius, R_h, may be calculated from the apparent diffusion coefficient using Stokes Einstein relationship. Interpreting L from R_h using Eq. (9) will result in an overestimate of the size of a semi-flexible molecule such as xanthan gum rotating in true Brownian motion.

The determination of c^* for semi-flexible molecules has received considerable interest in the literature, with a number of different equations being used directly for its calculation. Dynamic and Static Light Scattering techniques have been applied to investigate modified xanthan solutions, where c^* was calculated directly from the experimentally determined R_h using Eq. (10):

$$c^* = (3/4\pi) \times (M/Na_v R_h^3), \tag{10}$$

where M is the molecular weight. The authors (Coviello et al., 1986) recognised the difficulty in determining R_h for xanthan solutions reporting the overlapping of two apparent decay modes in the time correlation functions obtained from DLS. Tinland et al. (1990) defined c^* as the onset of interchain interaction when the average distance between the center of mass is equal to average chain extension (of order R_g). At c^* there is only one chain per volume R_g^3:

$$c^* = M_l \times L_c/R_g^3, \tag{11}$$

where M_l, L and R_g are the mass per unit length, contour length and the radius of gyration, respectively. The determination of R_g is a complicated process in the case of semi-flexible molecules. Prior work has shown that a third-order fit of the particle scattering function is required in the analysis of static light scattering data (Berth et al., 1996).

It is proposed here that c^* may be calculated by considering the R-squared end-to-end distance, $(\langle r^2 \rangle)^{1/2}$ of an individual molecule as being indicative of its effective hydrodynamic length as it rotates in Brownian motion, yielding Eq. (12):

$$c^* \times Na_v/M_w \cdot [(\langle r^2 \rangle 1/2]^3 = 1, \tag{12}$$

which is similar to that proposed in Eqs. (10) and (11). The determination of $\langle r^2 \rangle$ requires an experimental measure of persistence length (L_p) and the weight average molecular weight (M_w). The calculations follow the same procedure as previously done for xanthan gum (Tinland et al., 1990). The Benoit and Doty modification of the Krakty Porod model for a wormlike chain (Benoit & Doty, 1953) is used together with the inclusion of excluded volume effects to obtain an experimental persistence length (L_p). Eq. (13) is applied to calculate a value of $\langle r^2 \rangle$ assuming a molar mass

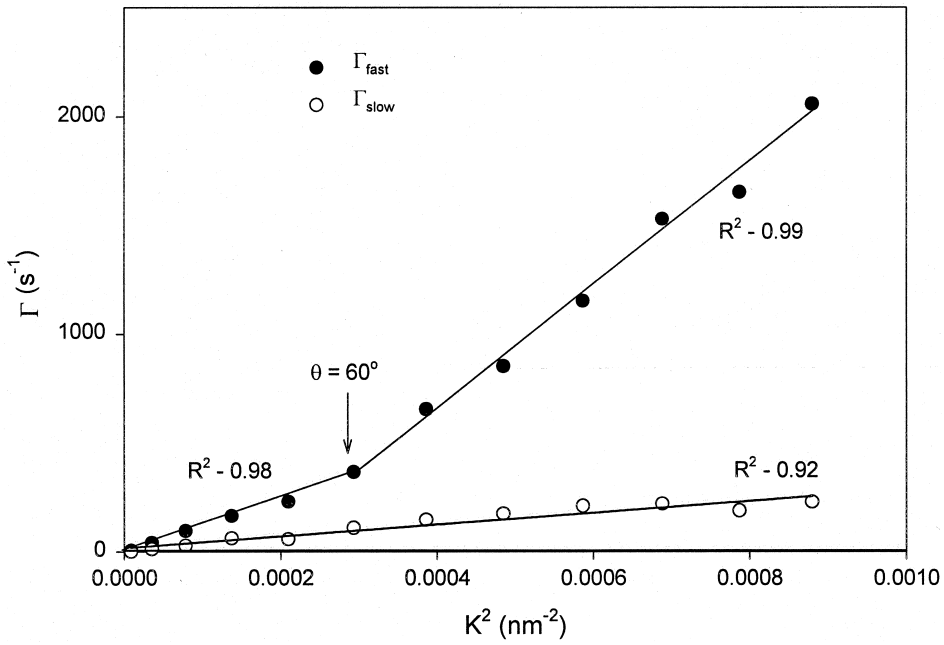

Fig. 5. $\bar{\Gamma}$ versus K^2 for xanthan in 15 000 ppm NaCl, measured at 25°C for a polymer concentration $c = 0.001$ wt%, $c^* < c < c^{**}$.

per unit length (M_l) of 1940 nm/(g mol^{-1}) and a pitch of 1.7 nm per repeat unit (Sato et al., 1984).

$$\langle r^2\rangle/L^2 = 2p(1 - p + p \times e^{(-1/p)}), \tag{13}$$

where L is the hydrodynamic length and $p = L_p/L$. Analysis of SLS data using the above procedure yielded a persistence length of 45 nm, which is in agreement with previous literature (Muller et al., 1984; Tinland et al., 1990; Tinland & Rinaudo, 1989). A considerable volume of work has shown L_p to be of the order of 120 nm (Berth et al., 1996; Sato et al., 1984) and therefore a value of $\langle r^2\rangle$ has been calculated for both. Application of Eqs. (12) and (13) yields a c^* for semi-flexible xanthan gum of 9.5×10^{-3} wt% and 19 Kuhn segment lengths for $L_p = 45$ nm and 2.4×10^{-3} wt% and seven Kuhn segment lengths for L_p of 120 nm. The number of Kuhn segment lengths, for both persistence lengths suggests that the behaviour of the xanthan molecule in solution should not approximate a rigid rod. The definitions of c^* presented above all require the determination of either R_g or R_h which, experimentally for xanthan gum solutions, is considered to be a non-trivial exercise. Table 1 presents c^* using the case of xanthan behaving as either a rigid rod or a semi-flexible molecule. All values calculated in each electrolyte condition were an order of magnitude below that observed rheologically.

The lower stress limit of the Carrimed CSL 100 is such that the low stress measurements may be obtained at Peclet numbers less than one (i.e., random Brownian motion dominates over imposed shear forces). For high aspect ratio rods and semi-flexible objects, there has been speculation as to whether the Peclet number is indicative of when the molecules are rotating randomly and unaffected by imposed hydrodynamics. Doi and Edwards (1984) present theoretical predictions suggesting that rods will be constrained to move longitudinally in a tube formed by their nearest neighbours before interactions occur. The alignment of rods caused by shear forces biases the apparent zero-shear viscosity, as the volume fraction of polymer in the direction of the shear would be reduced. The concept introduced by the Doi and Edwards (1984) constrained tube theory describes the properties of semi-flexible molecules qualitatively and therefore may describe the discrepancy between the c^* observed using rheological characterisation and the theoretically calculated values.

3.2. Dynamic light scattering results

DLS was conducted on solutions in a range of electrolyte concentrations. In order to ensure all measurements were made in the absence of time-dependent aggregation, samples were stored at 4°C after centrifugation for a minimum of three days. For each electrolyte concentration, xanthan concentrations between 0.5 and 1×10^{-6} wt% were measured.

To correctly characterise large aspect ratio molecules such as semi-flexible xanthan, it is important to investigate the angular dependence of diffusion data to determine the dependence of $\bar{\Gamma}$ with K^2. Fig. 5 illustrates such a plot of 0.001 wt% xanthan in 15 000 ppm NaCl for both cumulunts calculated using a CONTIN analysis of correlation functions obtained in series and parallel modes. The two observed linear regions for the fast mode are considered to be representing two individual diffusional modes that occur when molecules begin to interact. At dilute concentrations where no molecular interaction is observed and

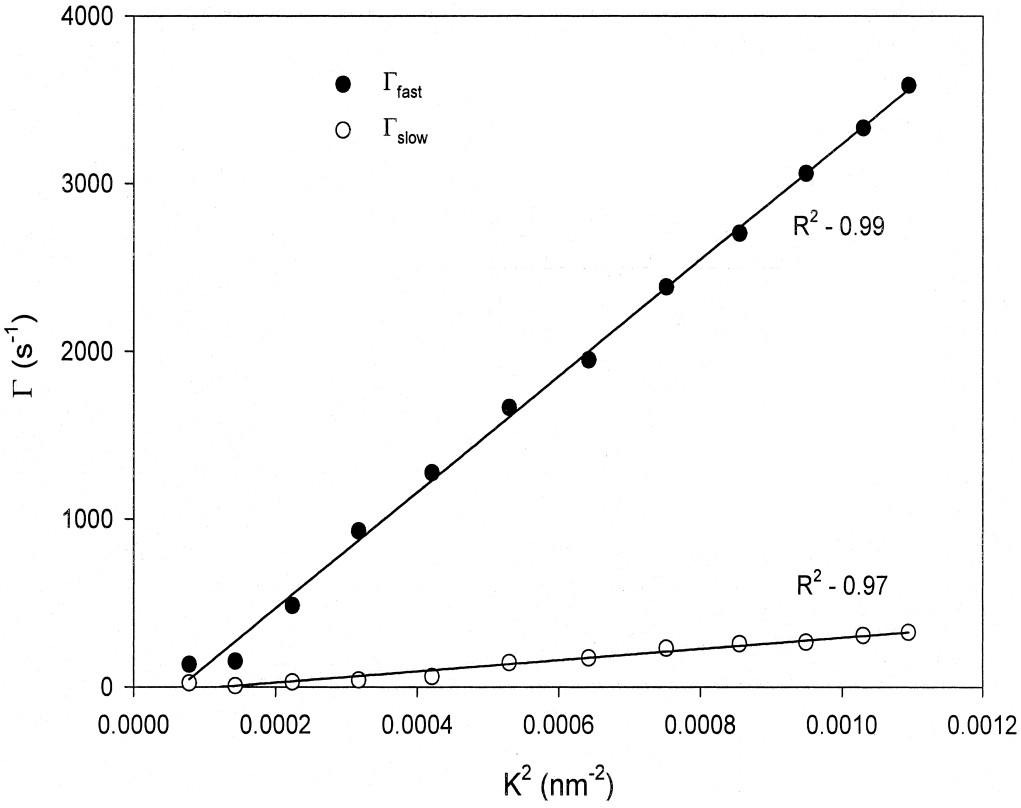

Fig. 6. $\bar{\Gamma}$ versus K^2 for xanthan in 15 000 ppm NaCl, measured at 25°C for a polymer concentration $c = 1 \times 10^{-5}$ wt%, $c < c^* < c^{**}$.

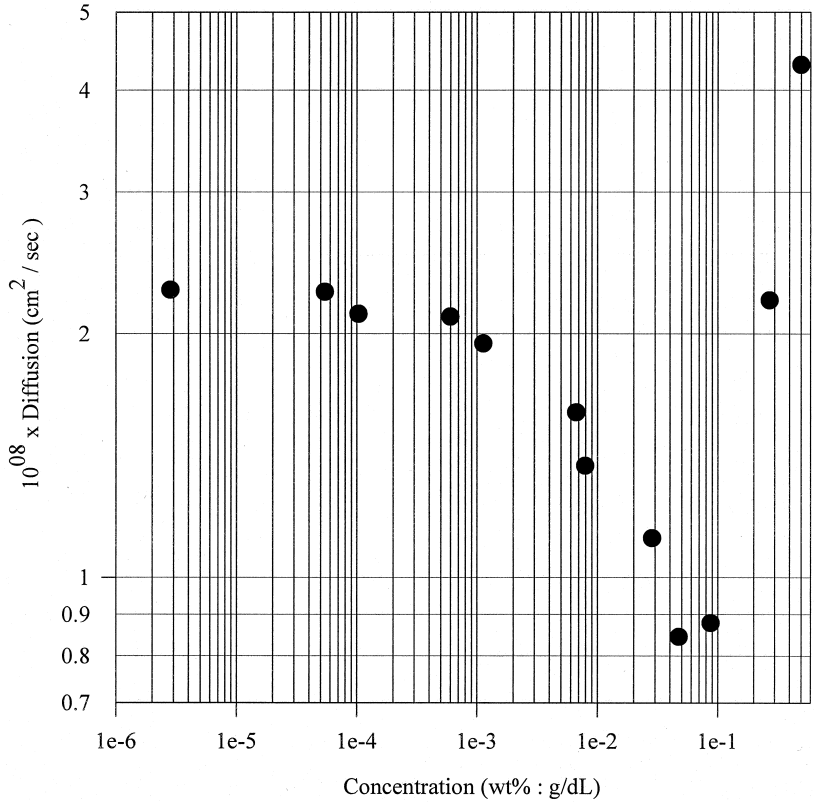

Fig. 7. Xanthan in 5000 ppm NaCl, Diffusion coefficient versus concentration at $\theta = 40°$.

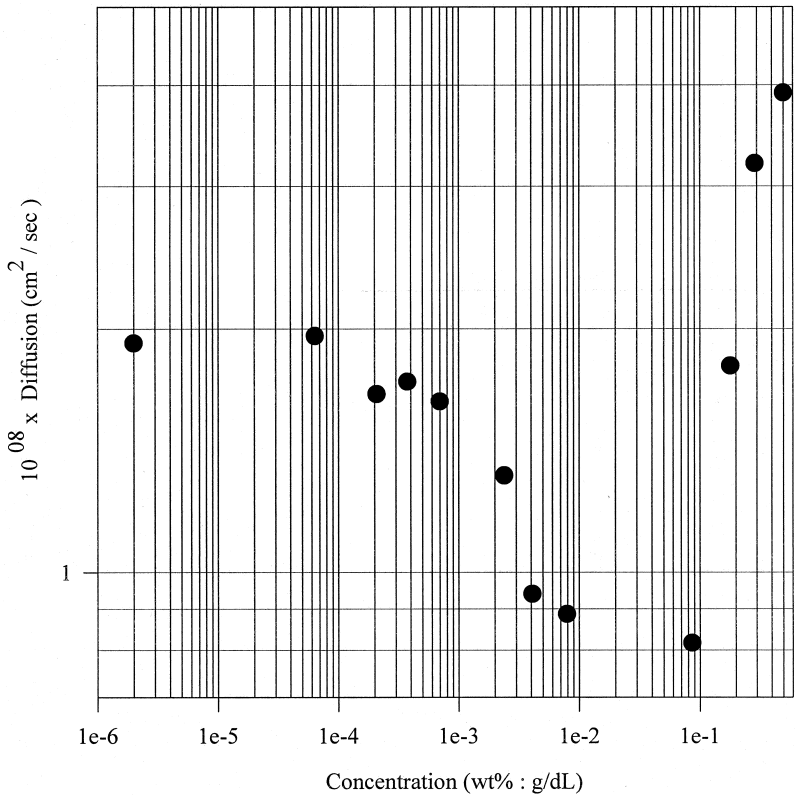

Fig. 8. Xanthan in 10 000 ppm NaCl, Diffusion Coefficient versus Concentration at $\theta = 40°$.

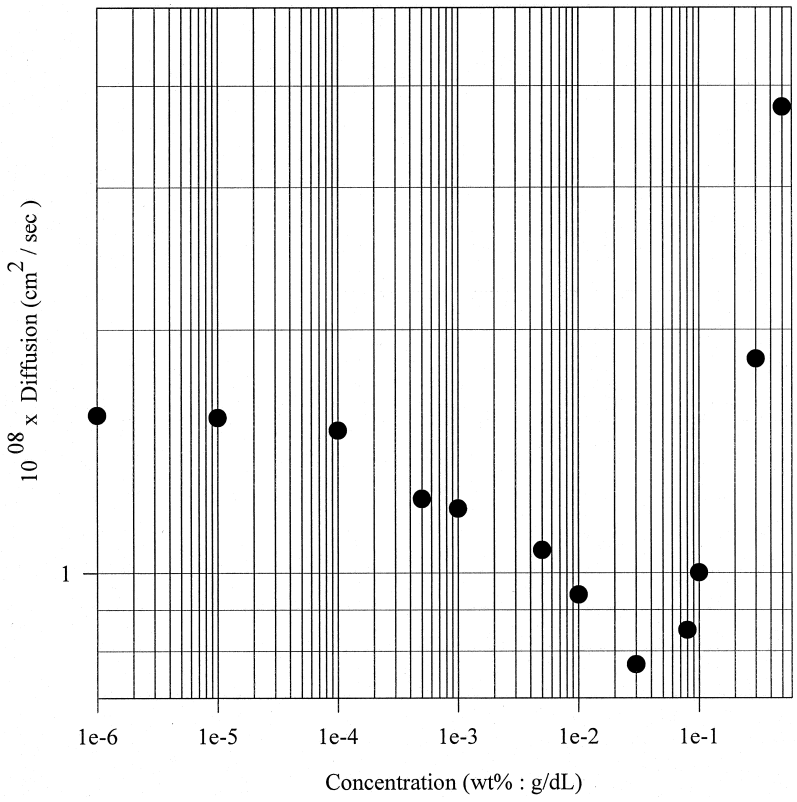

Fig. 9. Xanthan in 15 000 ppm NaCl, Diffusion Coefficient versus Concentration at $\theta = 40°$.

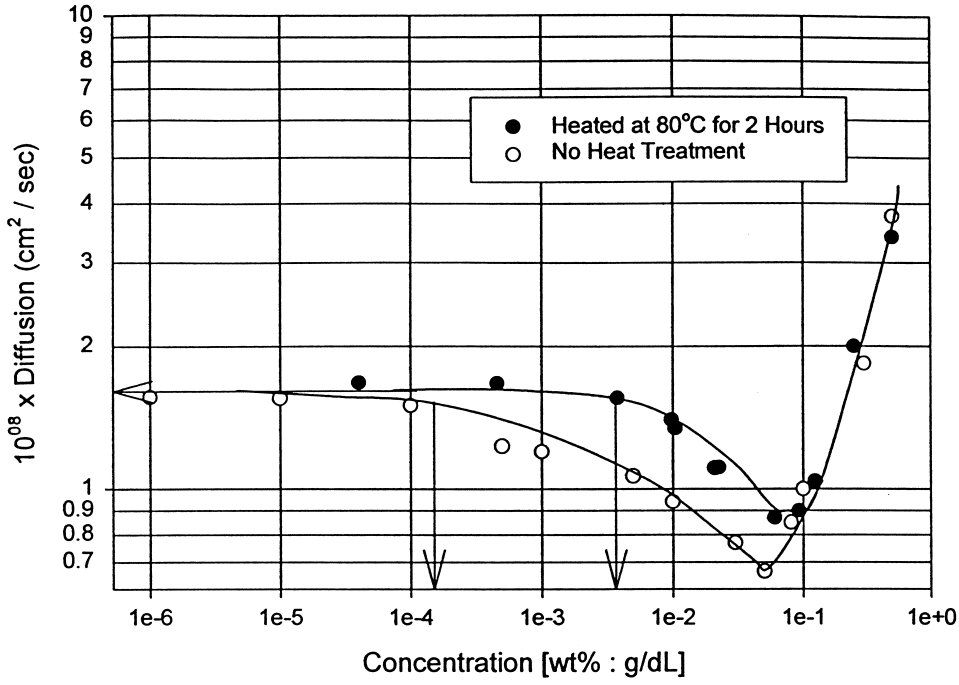

Fig. 10. Effect of heat treatment on measured diffusion versus concentration for xanthan solutions in 15 000 ppm NaCl. Scattering angle $\theta = 40°$. Heat treatment of 80°C for 2 h.

measured diffusion is independent of concentration, one linear region extends through all scattering angles as is illustrated in Fig. 6. For all concentrations and salt conditions, linearity was observed between scattering angles 15° of 60°.

The relative amplitudes of the fast and slow modes, as given by the values a_1 and a_2 in Eq. (4) were calculated as being constant at approximately 90:10 within experimental error and a fitting error of 0.004 ± 0.001 of the CONTIN analysis. The presence of a slow mode is consistent with previous work on xanthan gum. For the experiments conducted here, the slow mode was observed to be constant over the entire concentration range.

Figs. 7–9 show the measured diffusion coefficients as a function of xanthan concentration for the three electrolyte concentrations studied at a scattering angle of 40°. At infinite dilution all solutions show diffusion coefficients that plateau to a constant value, from which the hydrodynamic radius is calculated using the Stokes–Einstein equation. It is expected that as the concentration of molecules in solution increases, the volume in solution mapped out due to rotation in true Brownian motion will be such that they would be expected to overlap resulting in a reduction in the observed diffusion coefficient. The concentration at which the diffusion coefficient is estimated to vary by 5% from the infinitely dilute value, is allocated as the onset of interaction between molecules. Measured diffusion values for a range of concentrations from DLS are compared with the theoretically calculated values shown in Table 1.

The results from Table 1 show agreement, within the experimental error, of c^* between theoretical expectations for a solution of rigid rods and observed behaviour in a system in which shear forces are absent. It is important to note that these results are orders of magnitude lower in concentration than those previously reported (Gravanis et al., 1987; Meyer et al., 1993; Milas et al., 1990). From low shear viscometry Milas et al. (1990) report $c^* = 12.6 \times 10^{-3}$ wt% which agrees well with the theoretical predictions presented here with regard to calculations based on the Worm-like coil model and Jamieson et al. (1982) reports a c^* value of 20.0×10^{-3} wt%. It is proposed here that the deviation of diffusion from infinitely dilute behaviour at such low concentrations comes about because the samples were allowed to equilibrate for a number of days to allow for kinetics of aggregation to be complete. Aggregate formation has been previously reported to occur at low concentrations, 80 ppm (Southwick, Lee, Jamieson & Blackwell, 1980) and would therefore effect the concentration at which a deviation from dilute behaviour initially occurs.

In light of the well-reported processes of aggregation in solutions of xanthan gum, it is important to control the preparation of samples used in LS measurements. Heat treatment of the xanthan solutions has been avoided to ensure that the xanthan ordered structure is in its native form (Milas et al., 1996). Literature reports of the heat treatment of xanthan solutions have involved heating at 80°C under pressure for up to 2 h (Coviello et al., 1987). Milas et al. (1990) observed considerable effects in the viscosity profile of xanthan solutions through a range of concentrations after heat treatment of xanthan solutions at 80°C for only 1 min. Fig. 10 illustrates the effect of heat treatment of

xanthan at 80°C for 2 h on the diffusional measurements for xanthan in 15 000 ppm NaCl taken at a scattering angle of $\theta = 40°$. c^*, as observed by a deviation of diffusion from dilute solution behaviour, is raised considerably when the system has been subjected to heat treatment. The c^* calculated from Fig. 10 is approximately 5×10^{-3} wt% which is in reasonable agreement with the value calculated for a worm-like coil as listed in Table 1 for persistence lengths of 45 and 120 nm ($c^* \approx 9.0 \times 10^{-3}$ and 2.45×10^{-3} wt%, respectively). The increase in c^* is consistent with the heat treatment effectively removing xanthan aggregates and creating a true molecular dispersion.

In addition to the initial decrease in molecular diffusion caused by polymer–polymer interactions, at higher concentrations (0.07 wt%) a minimum in diffusion is observed, followed by a power law increase. It is proposed that the observed minimum is representative of a concentrated phase and represents the previously defined, critical concentration for aggregation (c^{**}).

3.3. Interpretation of dynamic light scattering data

The above discussion on the deviation from dilute behaviour, being indicative of c^* may be compared with the predictions for diffusivity for two extremities of molecular conformation, that of a random coil (De Gennes, 1979) and a rigid rod (Doi & Edwards, 1984). An increase in diffusion with increasing concentration at $c > c^{**}$ is argued theoretically to be caused by a concentrated phase dominating solution behaviour, with theoretical interpretations presented for both rigid rods and random coils.

Predictions of the dependence of diffusivity on concentration for rigid rods in solutions reported by Doi and Edwards (1984) provide a qualitative explanation for the observed behaviour. Theoretically, three of the four regimes defined by Doi and Edwards (1984) may be detected by analysing diffusivity trends. The four regimes for rigid rods predicted by Doi and Edwards (1984) consist of dilute, semi-dilute, isotropic concentrated and anisotropic concentrated. The isotropic concentrated solution and the semi-dilute solutions are not theoretically distinguishable by analysis of molecular diffusion. The dilute region is predicted to show no dependence of diffusion on concentration. Namely the number density concentration limitation suggested by Berry and Russel (1987) is not exceeded.

In the semi-dilute regions, the dominant interaction is the topological constraint that the polymers cannot cross each other. The motion along a polymer is almost free whilst the motion perpendicular to the direction of the polymers major axis is limited because of the presence of its nearest neighbours. In the semi-dilute regime, the diffusion dependence is modelled on a tube surrounding the test polymer. The radius of the tube (r) corresponds to the distance the polymer may move perpendicular to its own axis without being hindered by other molecules. The rotational diffusion is shown to follow the relationship:

$$D_r \simeq \frac{\left(\frac{r}{L}\right)^2}{\tau_d} \tag{14}$$

where L is the length of the molecule and τ_d is the average time required for the polymer to move outside its initial tube. As the concentration increases, according to Eq. (14), r will decrease as the individual molecules are restricted by their neighbours. Doi and Edwards (1984) proposed that this relationship would hold through the second and third concentration regimes. This concept qualitatively agrees with the initial decrease in diffusivity observed through the lower concentration regimes from DLS.

Previous observations of an initial deviation from dilute behaviour in xanthan solutions (Tinland et al., 1990), were explained in terms of reptation of semidilute solutions or worm-like polymers. The flexibility of the chain is accounted for by introducing the persistence length, L_p into the well-known expression for diffusion of flexible polymers in the semi-dilute regime, which follows:

$$D_s \cong (kT/\eta_0 a) \times n^{-2} \times c^{-7/4}, \tag{15}$$

where D_s is the measured diffusion coefficient, a is the monomer unit length, n is the number of monomer units and c is the polymer concentration (De Gennes, 1979). Tinland et al. (1990) presented simple scaling arguments for reptation behaviour of solutions of semi-flexible molecules by application of the De Gennes theory (1979) and conclude the diffusion in the semi-dilute regime should follow the relationship:

$$D_s = \frac{9kT}{8\pi\eta_0} \frac{1}{L_p^5 \cdot L_c^2} \times \left(\frac{M_L}{c}\right)^3 \tag{16}$$

Qualitatively, De Gennes (1979) predicted $D_s \propto c^{-3.5}$ for reptation in random coils, whilst the adaptation for a semi-flexible molecule presented by Tinland et al. (1990) predicted $D_s \propto c^{-3}$. Power law fits to the data reported in this work are much lower with $D_s \propto c^{-b}$ (b varying between 0.2 and 2). The scaling laws suggested do not consider the presence of anisotropic aggregates and are based on the concept of an average molecular weight between entanglements in solution.

Figs. 7–9 show diffusion decreasing with increasing polymer concentration, and then increasing after a pronounced minimum. Measurements in cells of varying diameter indicated that multiple scattering did not contribute to the observed trend. The results suggest a second transitional region has been observed which is predicted to be the onset of a region where anisotropic aggregates are present in solution, the transition being labelled c^{**} (Meyer et al., 1993; Milas et al., 1990). No theory is currently available to predict the properties of semi-flexible worm-like chains in semi-dilute solutions. Similar trends in

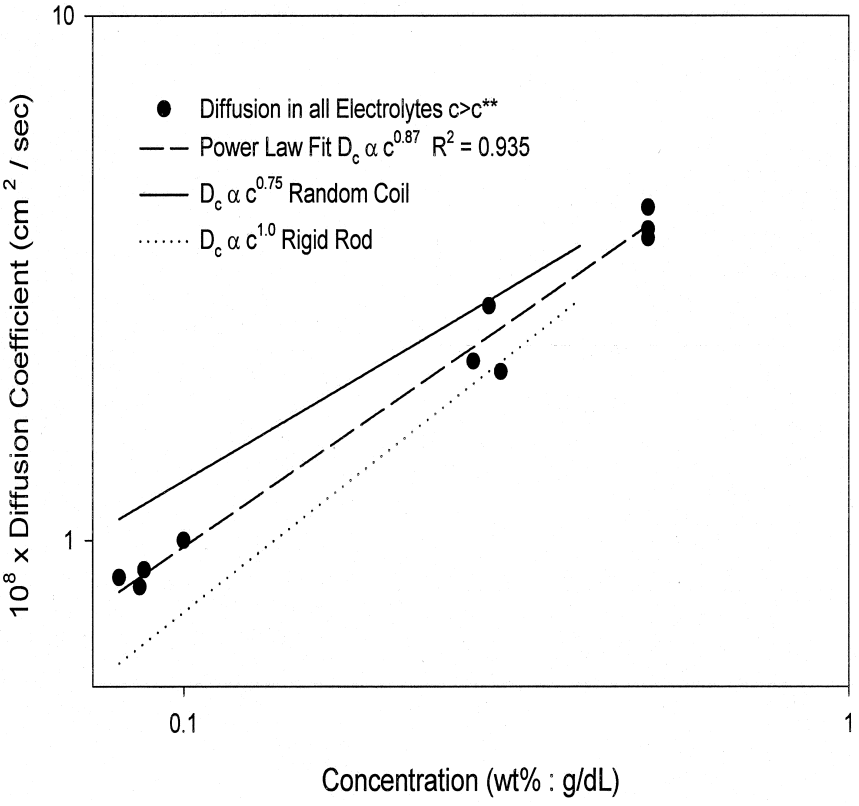

Fig. 11. Cooperative diffusion $D_{app} = D_c$ for xanthan in all electrolytes at $c > c^{**}$, power law fit. De Gennes (1979) predicts $D \propto c^{0.75}$ for flexible coils and Doi and Edwards (1984) predicts $D \propto c^{1.0}$.

the measured diffusion coefficients with concentration (Coviello et al., 1987; Tinland et al., 1990) have been described in terms of scaling concepts introduced by De Gennes (1979) for flexible chains in good solvents.

Doi and Edwards (1984) proposed for rigid molecules at higher concentrations, that a dispersed anisotropic phase was present. Here, static correlation of the polymers occurs in the absence of any external field. Doi and Edwards (1984) approximated the effect by proposing that, as a local area of polymers orientate in the one direction, the average diameter of the tube surrounding the test polymer increases. This concept is termed tube dilation. The result of tube dilation is to increase the rotational diffusion in the system for individual anisotropic domains and eventually for the entire solution as more of the molecules in their equilibrium state exist as part of the anisotropic domain. The existence of anisotropic domains has been observed experimentally over a large range of concentrations by a number of authors previously using rheological and spectroscopic techniques (Meyer et al., 1993; Milas et al., 1990; Milas et al., 1996). Doi and Edwards (1984) predicted the effect of tube dilation by orientational ordering on the diffusivity in solution, by considering the difference in orientation between the test polymer, its neighboring polymers and the overall approximated orientational distribution function of surrounding polymers. The result agrees qualitatively with the prediction of an increasing observed diffusivity due to tube dilation. The minimum observed in diffusivity as shown in Figs. 7–9, occurs at approximately the same concentration of 0.07 wt%. It is proposed that the minimum in diffusion represents a minimum concentration at which an anisotropic phase dominates solution behaviour at equilibrium. A value of $c^{**} = 0.07$ wt% is lower than that observed by Meyer et al. (1993) of $c^{**} = 0.2$ wt%, and Milas et al. (1990), $c^{**} = 0.6$–0.78 wt%. A value of c^{**} of 0.07 wt% is in agreement with a second concentration transition observed by Southwick et al. (1981) using flow birefringence. Both Meyer et al. (1993); Milas et al. (1990) suggested that the second concentration transition, c^{**} was due to the onset of anisotropic aggregation.

The increase in diffusion above a critical concentration herein denoted c^{**} has also been observed for polystyrenes of varying molecular weights in a θ solvent (Munch, Hild & Candau, 1983). Munch et al. (1983) observed a minimum in diffusion as a function of concentration when the fast mode of DLS results were considered.

The minimum in diffusion was explained by two competing modes to molecular diffusion. The initial decrease in diffusion is associated with hydrodynamic interactions, which results in a reduction of the translational self-diffusion coefficient. In the entangled solution (i.e. $c \gg c^*$ for a random coil system) the longer timescale (slower diffusion) motions are thought to be a result of cooperative chain diffusion. Munch et al. (1983) applied

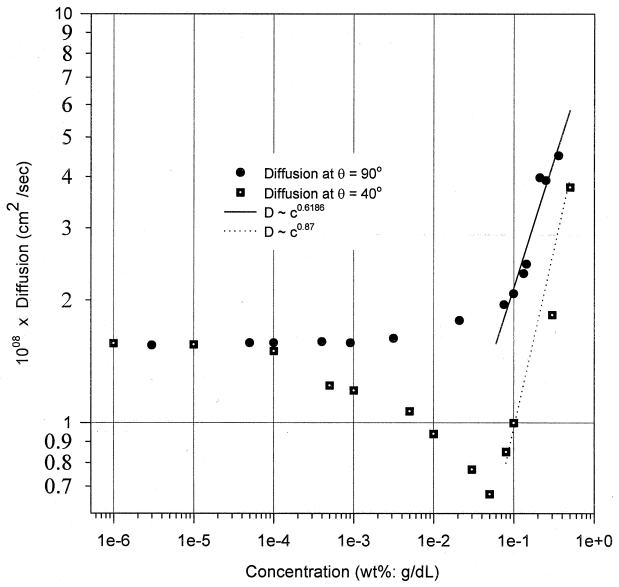

Fig. 12. Diffusion coefficient versus concentration for xanthan in 15 000 ppm NaCl. Measured at two scattering angles $\theta = 40°$ and $\theta = 90°$. Absence of minimum consistent with trend of first cumulunt, $\bar{\Gamma}$ with scattering vector K^2, reported in Figs. 5 and 6.

the theoretical predictions of Brochard and De Gennes (1977) to obtain an expression for diffusion at concentrations of $c \gg c^*$. Combining these predictions with observations by Munch et al. (1983) that the infinitely dilute diffusion coefficient D_0, varies as $M^{(-1/2)}$, the following expression is obtained:

$$D/D_0 = \beta c M^{1/2}, \tag{17}$$

where M is the molecular weight, c is the concentration and β is a numerical constant. The concept of c^* as described by Munch et al. (1983) could qualitatively be applied to a discussion for semi-rigid solutions where, at a critical concentration, cooperative chain diffusion arising from the formation of aggregates dominates solution behaviour.

A more detailed discussion of cooperative chain diffusion as applied to xanthan gum solutions is presented by Coviello et al. (1987). Munch et al. (1983) apply De Gennes (1979) and approximate xanthan solutions to contain entanglements of flexible chains and not the dispersed anisotropic phases as has been shown experimentally. An important quantity, the *correlation length*, ξ, is introduced at concentrations of $c \gg c^*$. The correlation length may be interpreted as the mean distance between two points of entanglements (De Gennes, 1979).

The diffusional behaviour in semidilute solutions is expected to be governed by the cooperative diffusion (D_c) given by a modified version of the well known Stokes–Einstein relationship to include the hydrodynamically defined correlation length, ξ_h:

$$D_c = kT/(6\pi\eta_0\xi_h). \tag{18}$$

The hydrodynamically defined correlation length is given by:

$$\xi_h = R_h \times (c/c^*)^{-(3/4)}. \tag{19}$$

Coviello et al. (1986); Coviello et al. (1987) derived Eqs. (18) and (19) from scaling arguments first presented by De Gennes (1979). Combination of Eqs. (18) and (19) and the Stokes–Einstein equation yields:

$$D_c/D_0 = (c/c^*)^{3/4} \propto c^{0.75}, \tag{20}$$

where D_0 is the diffusion representative of a single molecule in a dilute solution. Coviello et al. (1987) found that diffusion coefficients for xanthan in solution extrapolated to a zero angle showed increases in D_c/D_0 which were less than that predicted by the arguments above.

The scaling arguments of De Gennes (1979) derived for a transient network of random coil polymers, may be applied to concentrations above c^{**} where it is predicted that anisotropic aggregates dominate solution behaviour. Power law fits of the data yield an exponent of 0.87 that is independent of electrolyte concentration as shown in Fig. 11. It should be noted that the determined exponent of 0.87, is larger than 0.75 as predicted by De Gennes (1979) for random coil systems. However, it is less than the prediction of 1.0 for rigid rods (Doi & Edwards, 1984). Due to the semi-flexible nature of xanthan solutions, it is not conclusive that the results may be analysed by the introduction of correlation lengths between entanglements as it is well established that anisotropic domains are responsible for xanthan solutions behaviour at high concentrations. In addition, from the static light scattering results, a persistence length of $L_p = 45$ nm is determined resulting in 19 Kuhn Statistical Segment Lengths (L_k), where $L_k = 2 \times L_p$, suggesting that the formulae presented for Rigid Rods (Doi & Edwards, 1984) are also not applicable quantitatively.

A power law exponent of 0.87 is larger than 0.60 ± 0.02 as observed by Coviello et al. (1987). The difference may be attributed to the limitation of concentrations above c^{**} being considered in this work, whereas c^{**} was not a quantity characterised in the work of Coviello et al. (1987).

The measured diffusion coefficient as shown in Figs. 5 and 6, have two distinct regions of linearity in $\bar{\Gamma}$ versus K^2 when the xanthan concentration is above c^*. This trend was observed for all electrolyte concentrations studied, with the second linear region being between approximately 60 and 100° scattering angle. The diffusion coefficient measured at 90° is the same as that observed in second linear region.

Fig. 12 illustrates the trend in diffusion coefficient for xanthan solutions measured at an angle of 40° and secondly at 90°. The absence of the minimum in diffusion versus concentration for measurements conducted at 90° suggests that for scattering vectors over the range 60 to 100°, no initial decrease in diffusion predicted to be representing reptation for random coils or to topological constraints on rigid rods is observed. Although no initial decrease in

diffusion is observed, the higher concentration behaviour predicted to be either caused by tube dilation or cooperative diffusion observed in both angular ranges. Fig. 12 suggests that the power law exponent, determined from $c > c^{**}$, is dependent on how the angular range diffusion measurements are interpreted. The lower angle measures of diffusion are considered to be equivalent to zero angle diffusion measurements by extrapolation of data over a single linear range ($\theta = 20$–$60°$). A power law fit of the higher concentration diffusion data as measured at 90° yields an exponent of 0.62 which agrees with the coefficient as determined by Coviello et al. (1987) of 0.60 ± 0.02; however, is lower than the theoretically predicted 0.75 of De Gennes (1979). A scattering angle of $\theta = 40°$ gave a power law coefficient of 0.87. The diffusional measurements at 90° underestimate the power law predicted by the scaling arguments of De Gennes (1979), whereas measurements at 40° overestimates the power law dependence. As suggested by previous workers (Coviello et al., 1986), because of the semi-flexible nature of xanthan molecules, the scaling theory of De Gennes (1979) is not expected to fit quantitatively.

The absence of a minimum in diffusion at scattering vectors above $\theta = 60°$ and below $\theta = 100°$, suggests the diffusion representative of reptation for random coils or topological constraints for rigid rods is not observed. With further investigation of the angular dependence and interpretation of the scattering vector, it is postulated that the molecular origin of the measured diffusion coefficients may be determined.

4. Conclusions

DLS has been used to quantify two critical concentrations, the introduction of molecular interactions (c^*) and the onset of anisotropic aggregation (c^{**}), for solutions of semi-flexible xanthan gum. Both c^* and c^{**} have been determined by DLS in the absence of imposed shear forces. Results obtained from shear rheology give a biased measure of the introduction of molecular interaction (c^*) thought to be caused by the alignment of the molecules. Xanthan gum, reported to be a semi-flexible molecule, is compared with the theoretical predictions of molecular diffusion for both rigid rods (Doi & Edwards, 1984) and random coils (De Gennes, 1979). Initial interactions of molecules are indicated by a decrease in diffusivity, a trend predicted theoretically for topological constraints in constrained tubes (Doi & Edwards, 1984) as well as reptation for random coil molecules (De Gennes, 1979). Theoretical predictions for c^* based on $\langle r^2 \rangle$ calculated from the Benoit and Doty modification of the Krakty–Porod model for a wormlike chain were correlated only with samples having undergone a heat treatment, suggesting heat treatment to be critical in obtaining true molecular dispersions in the dilute regime. At higher concentrations a power law increase of diffusion was observed with concentration suggesting the onset of a second critical regime transition. A power law increase in diffusion is predicted for random coils in terms of cooperative diffusion arising from a correlation length and for rigid rods caused by static correlation of molecules under the influence of no external shear field. The power law dependence of the calculated diffusion coefficient for xanthan solutions was found to lie between the predictions for random coils and rigid rods. The onset of a power law dependence in diffusion was allocated c^{**} (critical concentration for aggregation), a quantity observed previously for xanthan solutions and determined in this study to occur at 0.07 wt% independent of electrolyte concentration used. The angular dependence of $\bar{\Gamma}$ versus K^2 illustrates the presence of two distinct diffusional modes dependant on the scattering angle range analysed. For angles less than 60°, zero angle diffusion could be extrapolated from a linear fit of $\bar{\Gamma}$ versus K^2. At scattering angles between 60 and 100° a second linear region in $\bar{\Gamma}$ versus K^2 is found, suggesting another diffusional mode is being observed. In the higher scattering angle region, no initial decrease in diffusion is observed suggesting that reptation of coils or topological constraints of rods may not be probed. At higher concentrations, a power law increase in diffusion is observed for both angular ranges, suggesting the effects of anisotropic aggregation may be seen. A similar analysis of various molecular weight xanthan molecules will establish the effect of xanthan flexibility as the number of statistical Kuhn segments is varied, on the observed diffusional trend and help to establish the origin of the observed molecular diffusion.

Acknowledgements

Andrew Rodd gratefully acknowledges the assistance of the Commonwealth Australian Postgraduate Award Scholarship, and the Cooperative Research Centre for Industrial Plant Biopolymers. A Special Investigation Grant, from the Australian Research Council awarded to David Boger is acknowledged.

References

Barnes, H. A., Hutton, J. F., & Walters, K. (1989). *An introduction to rheology*, Amsterdam: Elsevier.

Benoit, H., & Doty, P. (1953). Light scattering from non-gaussian chains. *Journal of Physical Chemistry, 57*, 958–963.

Berth, G., Dautzenburg, H., Christensen, B. E., Harding, S. E., Rother, G., & Smidsrod, O. (1996). Static light scattering studies on xanthan aqueous solutions. *Macromolecules, 29*, 3491–3498.

Berry, D. H., & Russel, W. B. (1987). The rheology of dilute suspensions of slender rods in weak flows. *Journal of Fluid Mechanics, 180*, 475–494.

Bezemer, L., Ubbink, J. B., deKooker, J. A., Kuil, M. E., & Leyte, J. C. (1993). On the conformational transitions of native xanthan. *Macromolecules, 26*, 6436–6446.

Brochard, F., & Gennes, P. G. (1977). Dynamic scaling for polymers in theta solvents. *Macromolecules, 10* (5), 1157–1161.

Broersma, S. (1960). Viscous force constant for a closed cylinder. *The Journal of Chemical Physics*, *32*, 1632–1635.

Capron, I., Brigand, G., & Muller, G. (1997). Size exclusion chromatograph, Laser light scattering and Xanthan. About the Native and Renatured Conformation of Xanthan Exopolysachharide. *Polymer*, *38*, 5289–5295.

Carriere, C. J., Amis, E. J., Schrag, J. L., & Ferry, J. D. (1993). Dilute solution dynamic viscoelastic properties of xanthan polysaccharide. *Journal of Rheology*, *37*, 469–478.

Chauveteau, G. (1982). Rodlike polymer solution flow through fine pores: influence of pore size on rheological behavior. *Journal of Rheology*, *26*, 111–142.

Coviello, T., Kajiwara, K., Burchard, W., Dentini, M., & Crescenzi, V. (1986). Solution properties of xanthan. 1. Dynamic and static light scattering from native and modified xanthans in dilute solutions. *Macromolecules*, *19*, 2826–2831.

Coviello, T., Burchard, W., Dentini, M., & Crescenzi, V. (1987). Solution properties of xanthan. 2. Dynamic and static light scattering from semidilute solutions. *Macromolecules*, *20*, 1102–1107.

Coviello, T., & Burchard, W. (1997). Static and dynamic light scattering by a thermoreverible gel from rhizobium leguminosarum 8002 exopolysaccharide. *Macromolecules*, *30*, 2008–2015.

De Gennes, P. G. (1979). *Scaling concepts in polymer solutions*, London: Cornell University Press.

Dhami, R., Harding, S. E., Jones, T., Hughes, T., Mitchell, J. R., & To, K. (1995). Physio-chemical studies on a commercial food-grade xanthan—I. Characterisation by sedimentation velocity, sedimentation equilibrium and viscometry. *Carbohydrate Polymers*, *27*, 93–99.

Doi, M., & Edwards, S. F. (1984). *The theory of polymer dynamics*, Oxford: Clarendon Press.

Ferry, J. D. (1980). *Viscoelastic properties of polymers*, 3. New York: Wiley.

Galinsky, G., & Burchard, W. (1996). Starch fractions as examples for nonrandomly branched macromolecules. 2 behavior in the semidilute region. *Macromolecules*, *29*, 1498–1506.

Gamini, A., & Mandell, M. (1994). Physiochemical properties of aqueous xanthan solutions: static light scattering. *Biopolymers*, *34*, 783–797.

Gravanis, G., Milas, M., Rinaudo, M., & Tinland, B. (1987). Comparative behavior of the bacterial polysaccharides xanthan and succinoglycan. *Carbohydrate Research*, *160*, 259–265.

Holzwarth, G. (1978). Molecular weight of xanthan polysaccharide. *Carbohydrate Research*, *66*, 173–186.

Jamieson, A. G., Southwick, J. G., & Blackwell, J. (1982). Dynamic behaviour of xanthan polysaccharide in solution. *Journal of Polymer Science, Polymer Physics Edition*, *20*, 1513–1524.

Kojima, T., & Berry, G. C. (1988). Solution properties of xanthan. light scattering and viscometry on dilute and moderately concentrated solutions. *Polymer*, *29*, 2249–2260.

Koppel, D. E. (1972). Analysis of macromolecular polydispersity in intensity correlation spectroscopy: The method of cumulunts. *Journal of Physical Chemistry*, *57*, 4814.

Lapasin, R., Pricl, S., Paoletti, S., & Zanetti, F. (1990). Novel rheological model for the gelation kinetics of ionic polysaccharides. *Journal of Applied Polymer Science*, *41*, 1395–1410.

Lapasin, R., & Pricl, S. (1993). *Rheology of industrial polysaccharides: theory and applications*, (pp. 38–39). London: Blackie Academic.

Mathiez, P., Mouttet, C., & Weisbuch, G. (1980). On the nature of the slow modes appearing in quasi-elastic light scattering by semi-dilute polymer solutions. *Journal de Physique*, *41*, 519–523.

Meyer, E. L., Fuller, G. G., Clark, R. C., & Kulicke, W.-M. (1993). Investigation of xanthan gum solution behavior under shear flow using rheooptical techniques. *Macromolecules*, *26*, 504–511.

Milas, M., Rinaudo, M., Knipper, M., & Schuppsier, J. L. (1990). Flow and viscoelastic properties of xanthan gum solutions. *Macromolecules*, *23*, 2506–2511.

Milas, M., Rinaudo, M., Duplessix, R., Borsali, R., & Lindner, P. (1995). Small angle neutron scattering from polyelectrolyte solutions: from disordered to ordered xanthan chain conformation. *Macromolecules*, *28*, 3119–3124.

Milas, M., Reed, W. F., & Printz, S. (1996). Conformations and flexibility of native and re-natured xanthan in aqueous solutions. *International Journal of Biological Macromolecules*, *18*, 211–221.

Milas, M., & Rinaudo, M. (1986). Properties of xanthan gum in aqueous solutions: role of the conformational transition. *Carbohydrate Research*, *158*, 191–204.

Morris, E. R., Morris, V. J., & Ross-Murphy, S. B. (1982). Molecular origin of xanthan solution rheology: effect of urea on chain conformation and interaction. *Journal of Polymer Science: Polymer Letters Edition*, *20*, 531–538.

Muller, G., Lecourtier, J., Chauveteau, G., & Allain, C. (1984). Conformation of the xanthan Molecule in the ordered structure. *Macromolecular Chemistry and Rapid Communication*, *5*, 203–208.

Munch, J., Hild, G., & Candau, S. (1983). Light spectroscopy in polymer solutions at theta conditions in the crossover concentration domain between the dilute and semidilute regimes. *Macromolecules*, *16*, 71–75.

Paradossi, G., & Brant, D. A. (1982). Light scattering studies of a series of xanthan fractions in aqueous solution. *Macromolecules*, *15*, 874–879.

Pecora, R., & Berne, B. J. (1976). *Dynamic light scattering*, New York: Wiley.

Provencher, S. W. (1979). Inverse problems in polymer characterization: direct analysis of polydispersity with photon correlation spectroscopy. *Makromolecule Chemistry*, *180*, 201–209.

Provencher, S. W. (1982). CONTIN: A general purpose constrained regularization program for inverting noisy linear algebraic and integral equations. *Computer Physics Communications*, *27*, 229–242.

Richards, E. G. (1980). *An introduction to the physical properties of large molecules in solution*, London: Cambridge University Press.

Rinaudo, M., & Milas, M. (1980). Enzymic hydrolysis of the bacterial polysaccharide xanthan by cellulase. *International Journal of Biological Macromolecules*, *2*, 45–48.

Ross-Murphy, S. B., Morris, V. J., & Morris, E. R. (1983). Molecular viscoelasticity of xanthan polysaccharide. *Faraday Symposium of the Chemical Society*, *18*, 115–129.

Sato, T., Norisuye, T., & Fujita, H. (1984). Double-stranded helix of xanthan: dimensional and hydrodynamic properties in 0.1 m aqueous sodium chloride. *Macromolecules*, *17*, 2696–2700.

Southwick, J. G., Lee, H., Jamieson, A. M., & Blackwell, J. (1980). Self-association of xanthan in aqueous solvent-systems. *Carbohydrate Research*, *84*, 287–295.

Southwick, J. G., Jamieson, A. M., & Blackwell, J. (1981). Quasi-elastic light scattering studies of semidilute xanthan solutions. *Macromolecules*, *14*, 1728–1732.

Stokke, B. T., Elgsaeter, A., & Smidsrod, O. (1986). Electron microscopic study of single- and double-stranded xanthan. *International Journal of Biological Macromolecules*, *8*, 217–225.

Tinland, B., Maret, G., & Rinaudo, M. (1990). Reptation in semidilute solutions of wormlike polymers. *Macromolecules*, *23*, 596–602.

Tinland, B., & Rinaudo, M. (1989). Dependence of the stiffness of the xanthan chain on the external salt concentration. *Macromolecules*, *22*, 1863–1865.

Whitcomb, P. J., & Macosko, C. W. (1978). The rheology of xanthan gum. *Journal of Rheology*, *22*, 493–505.

Wilkins, M. J., Davies, M. C., Jackson, D. E., Mitchell, J. R., Roberts, C. J., Stokke, B. T., & Tendler, S. J. B. (1993). Comparison of scanning tunneling microscopy and transmission electron microscopy image data of a microbial polysaccharide. *Ultramicroscopy*, *48*, 197–201.